Second-harmonic and third-harmonic generation in a three-component fibonacci optical superlattice

2000 J. Phys.: Condens. Matter 12 529

(http://iopscience.iop.org/0953-8984/12/5/301)

J. Phys.: Condens. Matter **12** (2000) 529–537. Printed in the UK PII: S0953-8984(00)03789-9

Second-harmonic and third-harmonic generation in a three-component fibonacci optical superlattice

Yan-bin Chen, Yong-yuan Zhu, Yi-qiang Qin, Chao Zhang, Shi-ning Zhu and Nai-ben Ming

National Laboratory of Solid State Microstructures and Department of Physics, Nanjing University, Nanjing 210093, China, and Center for Advanced Studies in Science and Technology of Microstructures, Nanjing 210093, China

Received 27 April 1999

Abstract. Harmonic generation in a three-component Fibonacci optical superlattice (3CFOS) is analysed theoretically. The Fourier spectrum of the structural function of the 3CFOS is numerically calculated. The positions of reciprocal vectors are in good agreement with the theoretical prediction. The intensities of the second harmonic (SH) and third-harmonic (TH) are calculated relative to the depletion of the fundamental. The dependence of the SH and TH intensity on structural parameters is discussed. Numerical calculation shows that, compared with two-component Fibonacci optical superlattice(2CFOS), there are more plentiful harmonic spectrum and adjustable structure parameters in 3CFOS. By chosen the reciprocal vectors and adjusted the structure parameters, the higher transform efficiency of THG is obtained.

1. Introduction

One of the most striking events in condensed-matter physics in the past 15 years has been the discovery of quasicrystals, which show many unusual physical properties [1]. Much effort has been devoted to the studies of structure and physical properties of quasicrystals [2, 3]. A quasiperiodic superlattice is an analogue of a one-dimensional quasicrystal. Merlin *et al* fabricated successfully the first quasiperiodic superlattice with molecular-beam epitaxy (MBE) in 1985 [4]. Since then many kinds of metallic and semiconductor quasiperiodic superlattice have been designed and produced by various techniques [5, 6]. In recent years a quasiperiodic superlattice has been realized in dielectric crystals, and the excitation and propagation of acoustic and optical waves have been studied both theoretically and experimentally [7–11]. For second-order nonlinear optical processes, the efficiency of parametric wave-mixing interactions can be enhanced significantly when the phase mismatches of optical parameter processes caused by the dispersion of the refractive index are compensated with the reciprocal vectors provided by the quasiperiodic dielectric superlattice [12–17]. Compared with the periodic dielectric superlattice, a quasiperiodic dielectric superlattice provides more reciprocal vectors due to its lower space-group symmetry. Because of this, not only the quasi-phase-matched (QPM) SHG, but also some coupled parameter processes, such as the THG and the fourth-harmonic generation (FHG), can be realized with high efficiency [18]. Until to now, however, these studies have been done only in the two-component Fibonacci optical superlattice (2CFOS). The 2CFOS consists of two building blocks A and B, each composed of a pair of oppositely polarized domains. A three-component Fibonacci superlattice (3CFOS) is a natural extension of the 2CFOS. It has three fundamental building blocks A, B and C.

0953-8984/00/050529+09$30.00

According to the theory of QPM, the similar optical parameter processes can also occur in a 3CFOS. Moreover, the reciprocal vectors of a 3CFOS are indexed with three integers, which means that more reciprocal vectors can be provided to participate in the QPM parameter processes in the superlattice, therefore, the harmonic spectrum structure of 3CFOS is more plentiful than a 2CFOS. This characteristic may be used to produce multi-wave-length QPM second harmonic and to design high-order harmonic device. In this paper, we will discuss the structure characterization of 3CFOS and present the theoretical results of QPM SHG and THG in the 3CFOS.

2. Theoretical analysis

A 3CFOS is constructed from three building blocks A, B and C, each composed of a pair of oppositely polarized domains. These fundamental blocks are shown in figure 1(a), where $l^+_{a\,(b,c)}, l^-_{a\,(b,c)}$ represent the thickness of the positive domain and the negative domain in block A (B,C) respectively. In this paper l^+_a is set to be equal to l^+_b and l^+_c ($l^+_a = l^+_b = l^+_c = l$) and $l_{a\,(b,c)}$ represents the length of the block A (B,C). The three types of block are arranged according to the following rule,

$$S_1 = \mathrm{A},\ S_2 = \mathrm{AC},\ S_3 = \mathrm{ACB}, \ldots, S_i = S_{i-1} * S_{i-3} \qquad (i \geqslant 4)$$

where $*$ stands for concatenation. The sequence ACBAACAC$\cdots$ produces a 3CFOS (see figure 1(b)).

As second-order nonlinear coefficients form a third-rank tensor, they change signs from the positive domain to the negative domain. For an infinite array, the quasiperiodically modulated effective nonlinear coefficient $d(x)$ can be written as, by use of the Fourier transform,

$$\frac{d(x)}{d_{33}} = f(x) = \sum_{m,n,l} f(G_{m,n,l})\, \mathrm{e}^{\mathrm{i}G_{m,n,l}x} \tag{1}$$

$$f(x) = \begin{cases} 1 & \text{if } x \text{ is in the negative domain} \\ -1 & \text{if } x \text{ is in the positive domain.} \end{cases}$$

$f(x)$ is called the structural function, which plays an important role in an optical superlattice. According to the projection method [19], the reciprocal vectors can be written as

$$G_{m,n,l} = \frac{2\pi(m\eta_1 + n\eta_2 + l\eta_3)}{D} \tag{2}$$

where m, n, l are integers, which label the reciprocal vectors. The set of η is defined as:

$$\eta_i = \lim_{n\to\infty}\left(\frac{|A_i|_n}{|A_1|_n}\right) \tag{3}$$

where A_i represents the ith type block, and $|A_i|_n$ represents the total number of A_i in the nth generation. It can be proved that η_i takes the following value:

$$\eta_2 = \tfrac{1}{3} + (\tfrac{29}{54} + \tfrac{1}{2}\sqrt{\tfrac{31}{27}})^{1/3} + (\tfrac{29}{54} - \tfrac{1}{2}\sqrt{\tfrac{31}{27}})^{1/3} \qquad \eta_3 = (\tfrac{1}{2} + \tfrac{1}{2}\sqrt{\tfrac{31}{27}})^{1/3} + (\tfrac{1}{2} - \tfrac{1}{2}\sqrt{\tfrac{31}{27}})^{1/3}$$

with $\eta_1 = 1$. D is the average parameter of the 3CFOS,

$$D = l_a\eta_1 + l_b\eta_2 + l_c\eta_3. \tag{4}$$

From equation (2) it can be seen that the position of a given reciprocal vector is only dependent on the average parameter. The $f(G_{m,n,l})$ in equation (1) can be expressed on the basis of the reverse Fourier transform as

$$f(G_{m,n,l}) = \frac{1}{\mathrm{i}LG_{m,n,l}} \sum_j \exp(\mathrm{i}G_{m,n,l}L_{j-1})[2\exp(\mathrm{i}G_{m,n,l}l^+_j) - 1 - \exp(\mathrm{i}G_{m,n,l}l_j)] \tag{5}$$

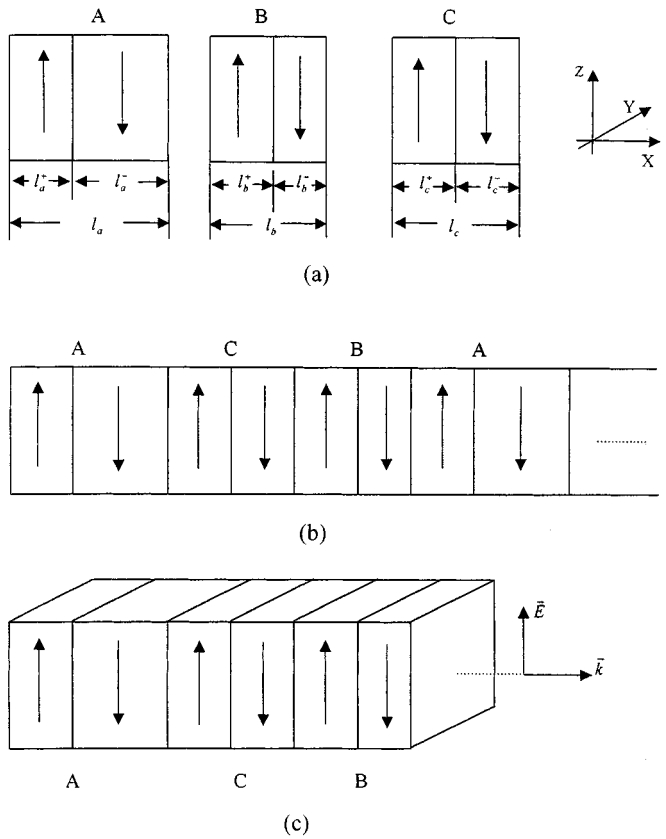

Figure 1. (a) The building blocks of the 3CFOS, A, B and C (the arrows indicate the direction of the spontaneous polarization). (b) A schematic diagram of a 3CFOS. (c) The polarization orientation of electric fields with respect to the superlattice.

where L is the total length of the optical superlattice and L_{j-1} is the total length of $j-1$ blocks. $l_j^+ = l_{a\,(b,c)}^+$, $l_j = l_{a\,(b,c)}$. From equation (5) the Fourier spectrum of the structural function is calculated as shown in figure 2. As shown in table 1, it can be seen that the numerical result is in good agreement with the theoretical analysis. It is easy to prove that the strongest peaks are those with $m{:}n{:}l \approx \eta_1{:}\eta_2{:}\eta_3$. This condition leads to the series of (m, n, l), which are the so-called general Fibonacci numbers (a_n, a_{n-2}, a_{n-1}). All of these (a_n) belong to the sequence described as $a_n = a_{n-1} + a_{n-3}$ with $a_1 = a_2 = 0$ and $a_3 = 1$. Then the strongest peaks satisfy

$$G(a_{n+3}, a_{n+1}, a_{n+2}) = G(a_{n+2}, a_n, a_{n+1}) + G(a_n, a_{n-2}, a_{n-1}) \tag{6}$$

which reflects the self-similarity of the Fourier spectrum.

In an optical superlattice, the most important physical processes are the excitation and the propagation of optical waves. In order to make use of the largest nonlinear coefficient d_{33} which cannot be used in an ordinary phase-matching regime, let the interfaces of each domain be parallel to the y–z plane, the optical wave propagate along the x axis and the direction of electric fields be along the z axis (see figure 1(c)). In this case the coupled nonlinear equations which describe the evolution of the slowly varying envelope for the fundamental, SH and TH

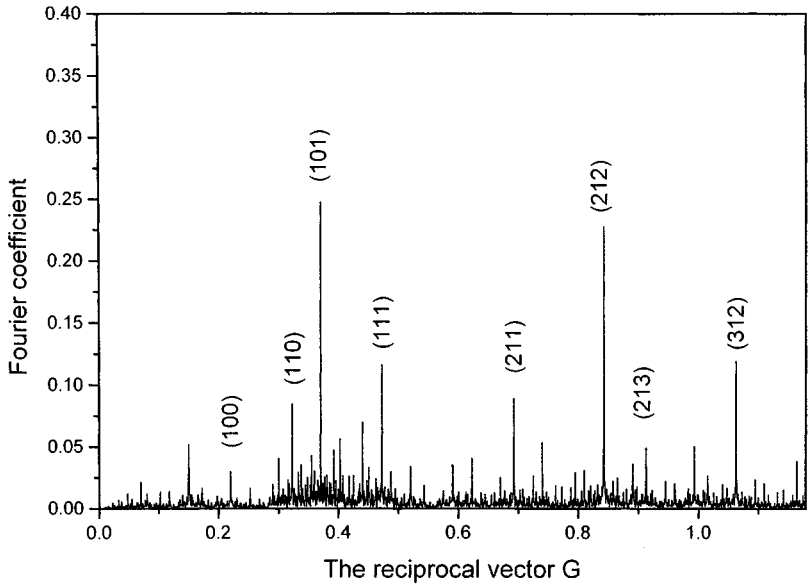

Figure 2. The Fourier spectrum of the structure function in 3CFOS with the structural parameters: $D = 28.564\ \mu$m, $l_a = 16.30\ \mu$m, $l_b = 6.52\ \mu$m, $l_c = 13.525\ \mu$m, $l = 3.50\ \mu$m. The strong peaks are indexed.

Table 1. Comparison between positions of the reciprocal vectors predicted by analysis and calculated by numerical method.

	(1, 0, 0)	(1, 1, 0)	(1, 1, 1)	(2, 1, 1)	(1, 0, 1)	(2, 1, 3)	(3, 1, 2)
Analytical prediction	0.219 96	0.322 38	0.472 47	0.692 44	0.370 06	0.992 62	1.062 50
Numerical calculation	0.219 75	0.322 31	0.472 59	0.692 34	0.370 04	0.992 44	1.062 38

electric fields are given by:

$$\begin{aligned}
\frac{\mathrm{d}E_1}{\mathrm{d}x} &= -\mathrm{i}\frac{\omega_1 d(x)}{n_1 c}E_3^* E_2 \exp(-\mathrm{i}\Delta k_2' x) - \mathrm{i}\frac{\omega_1 d(x)}{n_1 c}E_2^* E_1 \exp(-\mathrm{i}\Delta k_1' x) \\
\frac{\mathrm{d}E_2}{\mathrm{d}x} &= -\mathrm{i}\frac{\omega_2 d(x)}{2n_2 c}E_1^2 \exp(-\mathrm{i}\Delta k_1' x) - \mathrm{i}\frac{\omega_2 d(x)}{n_2 c}E_1^* E_3 \exp(-\mathrm{i}\Delta k_2' x) \\
\frac{\mathrm{d}E_3}{\mathrm{d}x} &= -\mathrm{i}\frac{\omega_3 d(x)}{n_3 c}E_1 E_2 \exp(\mathrm{i}\Delta k_2' x)
\end{aligned} \tag{7}$$

where n_1, n_2, n_3 are the refractive indices of the fundamental, SH and TH, respectively; $\omega_{1\,(2,3)}$ is the angular frequency of the fundamental (SH, TH); c, the speed of light in the vacuum;

$$\begin{aligned}
\Delta k_1' &= k_2 - 2k_1 = \frac{4\pi}{\lambda}(n_2 - n_1) \\
\Delta k_2' &= k_3 - k_2 - k_1 = \frac{2\pi}{\lambda}(3n_3 - 2n_2 - n_1).
\end{aligned} \tag{8}$$

k_1, k_2, k_3 represent the wavevector of the fundamental, SH and TH, respectively. , $\Delta k_1'$, $\Delta k_2'$ are the phase mismatches in SHG and the sum frequency generation process, respectively.

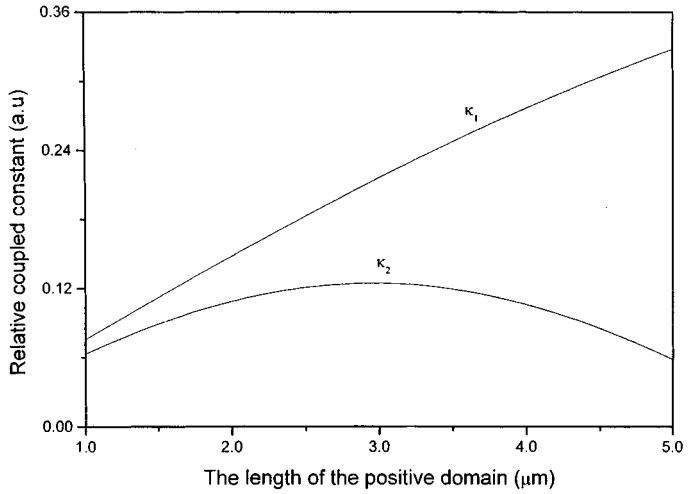

Figure 3. The dependence of the relative coupled constants κ_1, κ_2 on the positive domain length l. Other structural parameters are chosen as follows: $D = 28.564\ \mu$m, $l_a = 16.3\ \mu$m, $l_b = 6.52\ \mu$m, $l_c = 13.525\ \mu$m.

It is convenient to introduce a new field variable,

$$A_i = \sqrt{\frac{n_i}{\omega_i}} E_i \qquad i = 1, 2, 3. \tag{9}$$

By use of equations (1) and (9), equations (7) can be greatly simplified. In fact, only the Fourier component which is phase matched contributes significantly to the parametric interaction. If these non-phase-matched components are ignored, equations (7) become

$$\begin{aligned}
\frac{\mathrm{d}A_1}{\mathrm{d}x} &= -\mathrm{i}\kappa_2 A_3 A_2^* \exp(-\mathrm{i}\Delta k_2 x) - 2\mathrm{i}\kappa_1 A_2 A_1^* \exp(-\mathrm{i}\Delta k_1 x) \\
\frac{\mathrm{d}A_2}{\mathrm{d}x} &= -\mathrm{i}\kappa_2 A_3 A_1^* \exp(-\mathrm{i}\Delta k_2 x) - \mathrm{i}\kappa_1 A_1^2 \exp(\mathrm{i}\Delta k_1' x) \\
\frac{\mathrm{d}A_3}{\mathrm{d}x} &= -\mathrm{i}\kappa_2 A_2 A_1 \exp(\mathrm{i}\Delta k_2' x)
\end{aligned} \tag{10}$$

where κ_1, κ_2 are coupled constants,

$$\kappa_1 = \frac{d_{33} f(G_{m1,n1,l1})}{2c} \sqrt{\frac{\omega_1^2 \omega_2}{n_1^2 n_2}} \qquad \kappa_2 = \frac{d_{33} f(G_{m2,n2,l2})}{c} \sqrt{\frac{\omega_1 \omega_2 \omega_3}{n_1 n_2 n_3}}$$

and $\Delta k_1 = \Delta k_1' - G_{m1,n1,l1}$, $\Delta k_2 = \Delta k_2' - G_{m2,n2,l2}$.

It can be proved through derivation that

$$|A_1(x)|^2 + 2|A_2(x)|^2 + 3|A_3(x)|^2 = |A_1(0)|^2. \tag{11}$$

This is an equation of energy conservation in an optical superlattice. It shows that our approach is self-consistent. Equations (10) and the boundary conditions ($A_1(0) = 1$, $A_2(0) = 0$, $A_3(0) = 0$) compose the basis of our numerical calculation.

3. Numerical calculation and discussion

As it is shown in equations (10) that coefficients κ_1 and κ_2 determine the coupling strength of optical parameter process, in practice we must choose coefficients with high values. From the

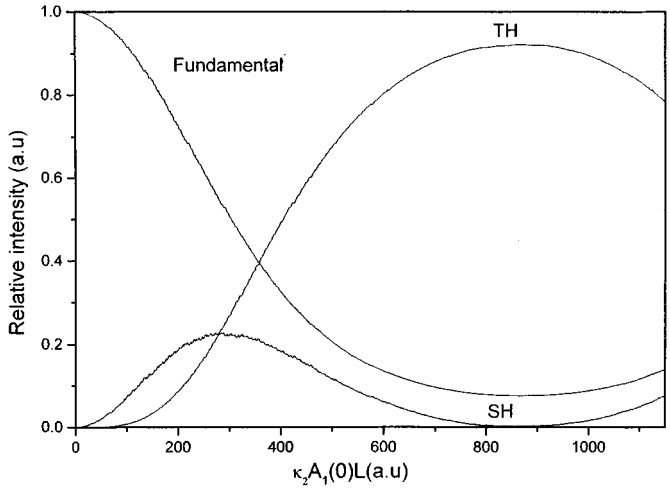

(a)

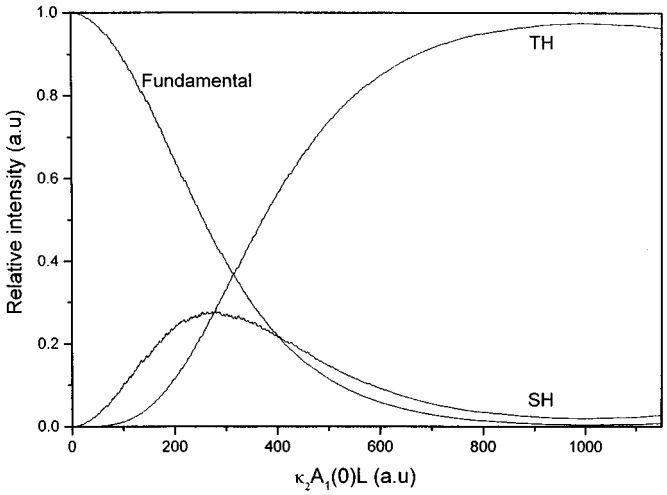

(b)

Figure 4. The dependence of the relative intensity of SH, TH and the fundamental on the non-dimensional length under different length of the positive domain. (a) $l = 2.5\ \mu$m; (b) $l = 3.0\ \mu$m; (c) $l = 3.5\ \mu$m. Other structural parameters are the same as those in figure 3.

expressions of κ_1 and κ_2, it can be seen that for a given fundamental wavelength the coupling constant is proportional to the corresponding Fourier coefficient $f(G)$. Here reciprocal vectors (3, 1, 2) and (1, 0, 1), which have higher weight in figure 2, are chosen to compensate the phase mismatch occurring in the THG and SHG. Therefore we obtain equations:

$$\Delta k_1 = \Delta k_1' - G_{1,0,1} = \frac{4\pi}{\lambda}(n_2 - n_1) - \frac{2\pi(1\cdot\eta_1 + 0\cdot\eta_2 + 1\cdot\eta_3)}{D} = 0$$
$$\Delta k_2 = \Delta k_2' - G_{3,1,2} = \frac{2\pi}{\lambda}(3n_3 - 2n_3 - n_1) - \frac{2\pi(3\cdot\eta_1 + 1\cdot\eta_2 + 2\cdot\eta_3)}{D} = 0. \qquad (12)$$

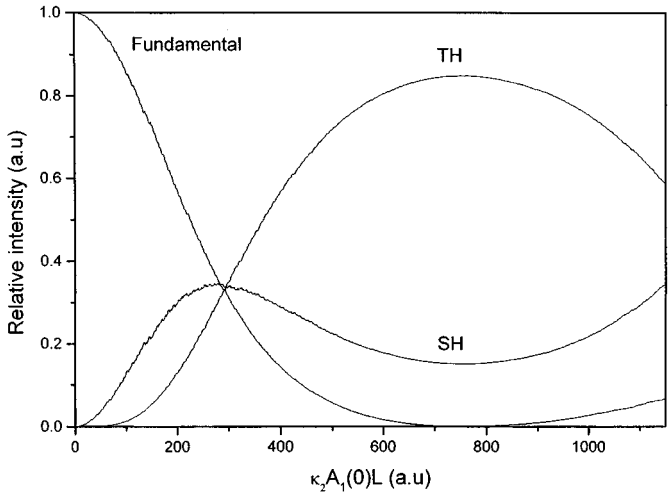

(c)

Figure 4. (Continued)

Because we want to gain the SH and TH in a single optical superlattice, the wavelength of the fundamental should be chosen to satisfy equations (12). We obtain the equation:

$$\frac{\eta_1 + \eta_3}{3\eta_1 + \eta_2 + 2\eta_3} = \frac{2(n_2 - n_1)}{3n_3 - 2n_2 - n_1}. \tag{13}$$

It can be calculated by using the refractive index data. Below we take $LiTaO_3$ (LT) crystal as an example [20]. At room temperature, when the wavelength of the fundamental is 1.4135 μm,

$$\begin{aligned} n_1 &= 2.126\,97 \qquad \lambda = 1.4135\ \mu\text{m} \\ n_2 &= 2.168\,56 \qquad \lambda/2 = 0.7068\ \mu\text{m} \\ n_3 &= 2.234\,40 \qquad \lambda/3 = 0.4712\ \mu\text{m} \end{aligned} \tag{14}$$

equations (12) could be satisfied perfectly,

$$\begin{aligned} \Delta k_1 &= -7.263 \times 10^{-7}\ \mu\text{m}^{-1} \\ \Delta k_2 &= -1.038 \times 10^{-7}\ \mu\text{m}^{-1}. \end{aligned} \tag{15}$$

Once the wavelength of the fundamental wave is given, the average parameter of the 3CFOS can be determined ($D = 28.564$ μm, when $\lambda_1 = 1.4135$ μm). In general, the lengths of building blocks and the positive domain are adjustable structural parameters, so long as equation (2) is satisfied. Below we discuss the effect of the structural parameters on the Fourier coefficient of the chosen reciprocal vector. Having compared with the Fourier spectrum with l_a, l_b, l_c taking various values, we find that when

$$l_a = 16.3\ \mu\text{m}, l_b = 6.52\ \mu\text{m}, l_c = 13.53\ \mu\text{m}$$

the Fourier coefficients $f(G_{3,1,2})$ and $f(G_{1,0,1})$ are fairly large in this case. So we take these values as structural parameters. Then we calculated the dependence of the coupling constants κ_1 and κ_2 on the length of the positive domain l (shown in figure 3). We found that the curve of κ_1 shows a monotonic dependence on the length of positive domain, whereas there is a maximum value in the curve of κ_2 at $l \approx 3$ μm. In order to see which value of κ_2 is appropriate for efficient THG, we choose three values of l around the maximum (2.5 μm, 3.0 μm and 3.5 μm) to calculate the intensity of harmonic beams.

Figures 4 show the dependence of relative intensity of the fundamental, SH, TH on the non-dimensional length $\kappa_2 A_1(0)L$ with l taking various values. These figures show the same tendency. That is, at first, the third harmonic grow more slowly than the second harmonic. After passing through a certain length of the superlattice, the third harmonic grows much faster. The reason for this is that the third harmonic depends strongly on the second harmonic. Also there are some differences among these figures. When the TH reaches its maximum, the remains of the fundamental and the SH are different. In figure 4(a) the maximum of the TH is accompanied by the exhaustion of the SH with some fundamental left, whereas in figure 4(c) the fundamental is used up with an appreciable SH remaining. When the structural parameter takes the value of 3.0 μm, the TH is the highest as shown in figure 4(b). In this case, both the fundamental and the SH are almost exhausted simultaneously.

The result obtained by numerical calculation is very different from the prediction through the small-signal approximation [18]:

$$I(3\omega) \propto (\kappa_1\kappa_2)^2$$

where $I(3\omega)$ is optical intensity ($I(3\omega) \propto |A(3\omega)|^2$). This means that the decisive factor to THG is the multiple of κ_1 and κ_2. But it contradicts the numerical calculation in which the most efficient THG does not take place when the multiple of κ_1 and κ_2 is the largest.

$$\kappa_1\kappa_2 = 0.022 \qquad l = 2.5\ \mu\text{m}$$
$$\kappa_1\kappa_2 = 0.027 \qquad l = 3.0\ \mu\text{m}$$
$$\kappa_1\kappa_2 = 0.030 \qquad l = 3.5\ \mu\text{m}.$$

The above numerical calculation indicates that with a larger κ_2, the THG might be generated much more efficiently. This may be a result of the fact that THG is a coupled parameter process. When the depletion of the fundamental is taken into account, the situation becomes complicated. As can be seen in equations (10), THG depends on κ_2 as well as the SH and the fundamental. Too large a value of κ_1 means a more efficient generation of SH, which may not be favourable to the THG, whereas a small value of κ_2 may lead to an inefficient THG (through the sum frequency generation). In the experiment, $\kappa_2 L$ is fixed, we can adjust $A_1(0)$ to obtain the most efficient THG.

4. Conclusion

In summary, we have investigated the THG and SHG in a 3CFOS with the depletion of the fundamental. The Fourier spectrum of the 3CFOS has been calculated, which shows the harmonic spectrum structure of 3CFOS is more plentiful than a 2CFOS. Through adjusting the structural parameters, efficient THG is obtained. The effect of the structural parameters on the efficient THG is also discussed. The method used here can be carried over to the other types of optical superlattice.

Acknowledgments

This work was supported by a grant from the State Key Program for Basic Research of China and by the National Natural Science Foundation of China.

References

[1] Shechtman D, Blech I, Gratias D and Cahn J W 1984 *Phys. Rev. Lett.* **53** 1951
[2] Steinhardt P J and Ostlund S 1987 *The Physics of Quasicrystals* (Singapore: World Scientific)

[3] Janot C 1992 *Quasicrystals* (Oxford: Clarendon)
[4] Merlin R, Bajema K, Clarke R, Juang F Y and Bhattacharya P K 1985 *Phys. Rev. Lett.* **55** 1768
[5] Birch J, Severin M, Wahlstrom U, Yamamoto Y, Radnoczi G, Riklund R and Walienberg L R 1990 *Phys. Rev.* B **41** 10 398
[6] Lu J P and Birman J L 1986 *J. Physique* C **3** 251
[7] Zhu Y Y and Ming N B 1992 *J. Appl. Phys.* **72** 904
[8] Xu H P, Jiang G Z, Mao L, Zhu Y Y and Qi M 1992 *J. Appl. Phys.* **71** 2480
[9] Feng J, Zhu Y Y and Ming N B 1990 *Phys. Rev.* B **41** 5578
[10] Zhu Y Y and Ming N B 1990 *Phys. Rev.* B **42** 3676
[11] Qin Y Q, Zhu Y Y, Zhu S N, Luo G P and Ming N B 1999 *Appl. Phys. Lett.* **75** 448
[12] Mizuuchi K, Yamamoto K and Kato M 1997 *Appl. Phys. Lett.* **70** 1201
[13] Armstrong J A, Bloembergen N, Ducuing J and Pershan P S 1962 *Phys. Rev.* **127** 1918
[14] Lin S J, Huang J Y, Ling J W, Chen C T, and Shen Y R 1991 *Appl. Phys. Lett.* **59** 2804
[15] Kang J U, Ding Y J, Burns W K and Melinger J S 1997 *Opt. Lett.* **22** 862
[16] Xu C Q, Okayama H and Kawahara M 1993 *Appl. Phys. Lett.* **63** 3559
[17] Hooper B A, Gauthier D J and Madey J M 1994 *Appl. Opt.* **33** 6981
[18] Zhu S N, Zhu Y Y and Ming N B 1997 *Science* **278** 843
[19] Hu A, Jiang S S, Peng R W, and Feng D 1992 *Acta Phys. Sin.* **41** 62
[20] Bond W L 1965 *J. Appl. Phys.* **36** 1674